IOP Publishing | Institute of Physics and Engineering in Medicine Physics in Medicine & Biology

Phys. Med. Biol. **60** (2015) 6639–6654 doi:10.1088/0031-9155/60/17/6639

Reference dosimetry in the presence of magnetic fields: conditions to validate Monte Carlo simulations

Hugo Bouchard[1], Jacco de Pooter[2], Alex Bielajew[3] and Simon Duane[1]

[1] Acoustics and Ionising Radiation Team, National Physical Laboratory, Hampton Road, Teddington TW11 0LW, UK
[2] VSL B.V., Thijsseweg 11, NL-2629 JA Delft, The Netherlands
[3] Department of Nuclear Engineering and Radiological Sciences, The University of Michigan, Ann Arbor, MI 48109, USA

E-mail: hugo.bouchard@npl.co.uk

Received 3 February 2015, revised 22 June 2015
Accepted for publication 26 June 2015
Published 13 August 2015

Abstract

With the advent of MRI-guided radiotherapy, reference dosimetry must be thoroughly addressed to account for the effects of the magnetic field on absorbed dose to water and on detector dose response. While Monte Carlo plays an essential role in reference dosimetry, it is also crucial for determining quality correction factors in these new conditions. The Fano cavity test is recognized as fundamental to validate Monte Carlo transport algorithms. In the presence of magnetic fields, it is necessary to define special conditions under which such a test can be performed. The present theoretical study proposes two conditions in which the validity of Fano's theorem is demonstrated in the presence of a magnetic field and the analytic expression of energy deposition is verified. It is concluded that the proposed conditions form a valid basis for two types of Fano cavity tests in the presence of a magnetic field.

Keywords: reference dosimetry, MRI-guided radiotherapy, Fano theorem, Fano cavity test, Monte Carlo radiation transport, magnetic fields, ionisation chamber response

(Some figures may appear in colour only in the online journal)

1. Introduction

Monte Carlo plays an important role in the calibration of radiotherapy machines. While ionisation chambers are usually calibrated for standard conditions (Almond *et al* 1999, Andreo

et al 2001), quality correction factors, which are meant to account for the dependence of calibration coefficients on beam quality, have been tabulated for standard beams based on Monte Carlo simulations (Andreo and Brahme 1986, Kosunen and Rogers 1993, Andreo 1994, Rogers and Yang 1999, Muir and Rogers 2010, Muir *et al* 2011, McEwen *et al* 2014). For nonstandard beams, such as small fields and modulated beams, these factors are also evaluated mostly with Monte Carlo methods (Alfonso *et al* 2008, Francescon *et al* 2008, Scott *et al* 2008, Francescon *et al* 2011, Cranmer-Sargison *et al* 2012, Francescon *et al* 2012, Gago-Arias *et al* 2012, Scott *et al* 2012, Sterpin *et al* 2012, Czarnecki and Zink 2013, Underwood *et al* 2013, Benmakhlouf *et al* 2014, Francescon *et al* 2014a, 2014b, Kamio and Bouchard 2014, Papaconstadopoulos *et al* 2014). With the advent of MRI-guided radiotherapy, the simulation of detector dose response to megavoltage photon beams in the presence of an external magnetic field is of increasing interest. Recent Monte Carlo studies showed that significant correction factors are expected for the calibration of MRI-guided radiotherapy machines when performed with ionisation chambers calibrated under standard reference conditions (Meijsing *et al* 2009, Reynolds *et al* 2013). However, the accuracy of the results reported in these studies remains debatable to this day, since no appropriate method to validate the simulations has yet been proposed. The recent publication by Smit *et al* suggested agreement between experimental and simulated ionisation chamber dose response in a MRI-linac prototype (Smit *et al* 2013) and proposed to adapt standard reference dosimetry techniques (Almond *et al* 1999, Andreo *et al* 2001) by correcting the chamber reading for the effect of the magnetic field on its response. This approach alone is potentially confusing. The chamber reading, once corrected for polarity and recombination effects, is the ionisation produced in the sensitive volume and does not need further corrections; what requires correction is the chamber calibration coefficient, and one needs to also account for the effect of the magnetic field on absorbed dose to water in the absence of the detector. Note that in general, the magnetic field could also have an effect on the detector yield (e.g. ion recombination, compatibility of alanine/EPR in magnetic fields, etc) and these effects are currently under investigation. Therefore, the accurate determination of quality correction factors (i.e. $k_{Q_B,Q}^{f_B,f}$), which account for the change in beam quality and its effect on the detector, is yet to be achieved with Monte Carlo and might require experimental data.

To benchmark Monte Carlo radiation transport algorithms, the Fano cavity test (or Fano test) is widely recognized as a major requirement, especially in the context of ionisation chamber dose response simulation. Based on Fano's theorem (Fano 1954), this test is the only known method allowing the validation of charged particle energy deposition in heterogeneous media against an analytic expression, this way testing the self consistency and implementation of the charged particle step algorithms, which is typically composed of a multiple scattering model and a boundary crossing algorithm (Kawrakow 2000a). The Fano test was first proposed by Smyth (1986) and further adapted by other authors in EGS4 (Bielajew 1990a, 1990b, Foote and Smyth 1995), EGSnrc (Kawrakow 2000b), PENELOPE (Sempau and Andreo 2006, Yi *et al* 2006) and GEANT4 (Poon and Verhaegen 2005, Elles *et al* 2008, Sterpin *et al* 2014). For detector dose response simulations, the level to which the Fano test is achieved is often interpreted as the accuracy of the code, to which a level of 0.1% was first reached with EGSnrc for cobalt-60 (Kawrakow 2000b) and electrons (Seuntjens *et al* 2002), later with PENELOPE for the same types of beam (Sempau and Andreo 2006, Yi *et al* 2006) and GEANT4 and PENH for proton beams (Sterpin *et al* 2014). By definition, the Fano test is applicable to a heterogeneous geometry where the properties are spatially uniform, such that the interaction cross sections are directly proportional to the mass density. The test requires a special condition on the primary source in order to obtain a spatially uniform charged particle fluence (a condition also known as charged particle equilibrium), either by simulating a parallel photon beam and

removing the effect of the beam attenuation (i.e. the regeneration technique (Bielajew 1990a, 1990b)), or by using an isotropic primary electron source being uniform per unit mass. The expected absorbed dose in any scoring region is then equal to the energy transferred to charged particle per unit mass from the primary source.

In the presence of an external magnetic field distribution, we recently showed that Fano's theorem (Fano 1954), on which Fano tests rely, cannot hold for arbitrary source and field distributions (Bouchard and Bielajew 2015). The work was initially presented at the International Workshop on Monte Carlo Techniques in Medical Physics in Québec City in 2014 (Bouchard and Bielajew 2014). One can intuitively understand why Fano's conditions could be violated in magnetic fields by representing a geometry of varying mass density subject to a uniform magnetic field. Since the field does not scale with the mass density, the magnetic force remains uniform (for given energy and direction), while the electron stopping power, also being a force, is proportional to the mass density. Therefore the ratio of the magnetic force over the stopping power is inversely proportional to the mass density, and so is the ratio of the electron range over the bending radius of the magnetic force. Although the magnetic force do no work, its bending effect on the electron trajectory results in fluence perturbations near the boundary of regions having distinctive mass densities. Therefore, in a varying-density geometry irradiated by a uniform and parallel photon source, which would establish charged particle equilibrium in the absence of a magnetic field, one should expect the electron fluence not to be uniform, unless special conditions are fulfilled.

The invalidity of Fano's theorem has the consequence of limiting our ability to validate the implementation of the Lorentz force in Monte Carlo codes simulating charged particle transport in dense matter. To develop an appropriate test under such new constraints, the Fano test must be adapted by defining conditions under which Fano's theorem is valid. Once established, special Fano tests will allow evaluating the accuracy of Monte Carlo codes coupled to magnetic fields, especially in the context of detector dose response simulation.

Based on the modified Boltzmann transport equation we proposed which accounts for the presence of external magnetic fields (Bouchard and Bielajew 2015), the present paper reports the theoretical investigation of two special conditions under which charged particle equilibrium can be established. Under these conditions, Fano's theorem is verified by demonstrating that the charged particle fluences are independent of mass density variations. An analytic expression for energy deposition is also obtained in agreement with the classical Fano test. This allows completing the design of two special Fano tests applicable in the presence of magnetic fields.

The paper is structured as follows. The next section provides relevant mathematical definitions to explore the theory of transport in the presence of magnetic fields. In the third section, the classical Fano theorem is described and it is explained in detail why it does not hold generally in the presence of magnetic fields. In the fourth section, the two special conditions are rigorously addressed from a theoretical point of view. Before concluding on the expected impact of this work, the energy deposition for the proposed special Fano tests are derived in the fifth section, showing perfect agreement of the analytic expression with classical Fano tests.

2. Definitions

- $\vec{r}$: a vector corresponding to the particle position in space (in cm), i.e. $\vec{r} = (x, y, z)$.
- $\vec{p}$: a vector corresponding to the particle momentum (in MeV s cm^{-1}), i.e. $\vec{p} = (p_x, p_y, p_z)$ and $p = |\vec{p}|$.
- $\vec{u}$: a unit vector in the direction of the particle momentum $\vec{p}$, i.e. $\vec{u} = \frac{\vec{p}}{p}$.

- t: the time (in s).
- s: the path travelled by the particle (in cm).
- $\rho \mathrm{d}s$: an infinitesimal step of mass-thickness trajectory (in g cm^{-2}).
- mass-thickness trajectory: particle trajectory in a homogeneous medium in terms of mass-thickness spatial coordinates. These coordinates are obtained by multiplying the spatial coordinates (x, y, z) by the mass density, i.e. ($\rho x, \rho y, \rho z$).
- β: the particle velocity relative to the speed of light.
- γ: the Lorentz factor defined as $\frac{1}{\sqrt{1-\beta^2}}$.
- mc^2: the particle rest mass energy (in MeV).
- T: the particle kinetic energy (in MeV). For photons, $T = pc$, and for electrons and positrons, $T = \sqrt{p^2c^2 - m^2c^4} - mc^2$.
- $f_i(\vec{r}, \vec{p})$: the fluence differential in energy and direction (in cm^{-2} MeV^{-1} sr^{-1}) of the particle type i (i.e. photons, electrons or positrons) corresponding to the number of particles at $\vec{r}$ with momentum $\vec{p}$ per unit energy, per unit area perpendicular to $\vec{u}$ and per unit solid angle $\mathrm{d}\vec{u} = \sin\theta \mathrm{d}\theta \mathrm{d}\phi$.
- $\sigma_{ji}(\vec{p}' \rightarrow \vec{p})$: the differential cross section per unit energy and solid angle (in cm^2 MeV^{-1} sr^{-1}) for a particle of type j with momentum $\vec{p}'$ to generate a particle of type i with momentum $\vec{p}$ through any interaction (i.e. photoelectric effect, Compton scattering, Mϕller scattering, etc). Note that the cross section can also be expressed as a function of the energy of the primary and secondaries, i.e. T' and T, as well as the cosine of the scattering angle $\cos\chi = \vec{u} \cdot \vec{u}'$.
- $\mu_i(p)$: the macroscopic cross section (in cm^2 g^{-1}) for a particle of type i with momentum p to interact locally with the medium.
- N: the number of interaction sites per unit mass (in g^{-1}).
- ρ: the mass density of the medium (in g cm^{-3}).
- $\vec{B}$: a position-dependent vector corresponding to the magnetic field (in T) at $\vec{r}$, i.e. $\vec{B} \equiv \vec{B}(\vec{r})$.
- $S_i(\vec{r}, \vec{p})$: the primary source term representing the number of particles of momentum $\vec{p}$ generated at $\vec{r}$ by an external source per unit mass, energy and direction (in g^{-1} MeV^{-1} sr^{-1}).
- $\vec{\nabla}_r$: the gradient operator in the space coordinates defined as $\vec{\nabla}_r = \hat{x}\frac{\partial}{\partial x} + \hat{y}\frac{\partial}{\partial y} + \hat{z}\frac{\partial}{\partial z}$.
- $\vec{\nabla}_p$: the gradient operator in the moment coordinates defined as $\vec{\nabla}_p = \vec{u}\,\frac{\partial}{\partial p} + \hat{\theta}\,\frac{1}{p}\frac{\partial}{\partial \theta} + \hat{\phi}\,\frac{1}{p\sin\theta}\frac{\partial}{\partial \phi}$.
- Spatial uniformity: this terminology is applied either to a mathematical function or to atomic properties. A mathematical function F is spatially uniform if and only if $\vec{\nabla}_r F = \vec{0}$. Atomic properties are spatially uniformity if physical properties of a given geometry, such as the mean excitation energy (I-value), the effective atomic number (or elemental composition) and the density effect parameter δ are uniform in space. This allows the macroscopic cross section of any interaction type to scale directly with the mass density.
- Isotropy: this terminology is applied to a mathematical function being independent on the particle direction (or angular distribution). A mathematical function F is isotropic if and only if $\frac{\partial F}{\partial \theta} = \frac{\partial F}{\partial \phi} = 0$ for all θ and ϕ.

3. Fano's theorem and its breakdown in external magnetic fields

In our previous approach (Bouchard and Bielajew 2015), we provided a formal proof of the statement that Fano's theorem cannot apply in the presence of external electromagnetic fields

unless special conditions are met. To illustrate this in more detail, it is worth representing Fano's theorem in such a way that presence of the Lorentz force requires special conditions for Fano's theorem to hold.

3.1. An alternative representation of the classical Fano theorem

In the absence of a magnetic field, Fano's theorem states the following (Fano 1954):

> *In a medium with uniform atomic properties irradiated by a source of primary particles being spatially uniform, the charged particle fluence is also uniform and independent of the mass density distribution.*

An intuitive proof of the theorem can be constructed by reformulating Fano's statement as follows:

> *In a medium where the charged particle mass-thickness trajectories are independent of the mass density and the source of primary particles irradiating the medium is spatially uniform, the charged particle fluence is also uniform and independent of the mass density distribution.*

Here the statement is modified by replacing the requirement of uniform atomic properties with the condition that the mass-thickness trajectories of secondary particles are independent of the mass density. These arguments are equivalent. The fact that the medium is defined to have spatially uniform atomic properties means that the macroscopic cross sections of all physical interactions are directly proportional to the mass density, and therefore one can represent mass-thickness trajectories independently of the mass density. Equivalently, charged particle mass-thickness trajectories can only be independent of the mass density if the medium atomic properties are uniform. Therefore if one describes the change in energy and direction of the particle as a function of its path in of terms of mass thickness, the equations of motion are independent of the mass density distribution.

Let us show that this rationale applies in the cases of energy loss and scattering. Charged particle stopping power can be written in terms of mass thickness as follows:

$$\frac{\mathrm{d}T}{\rho \mathrm{d}s} = -S_m(T), \tag{1}$$

where S_m is the mass stopping power. As S_m is independent of the mass density (keeping the density effect parameter aside), this equation of motion describing the mass-thickness trajectory is also independent of the mass density. Note that for a given material, the density effect parameter δ varies with the mass density, and therefore Fano tests must be applied with spatially uniform values at each energy (e.g. δ of vapor is replaced by δ of water).

Charged particle scattering angles are also independent of the mass density, fundamentally because particle directions represent relative coordinate displacements in a given frame of reference. Representing the particle mass-thickness trajectory, each dimension of the trajectory is equally scaled and therefore the scattering angle is independent of the mass density. This can be further illustrated using the example of multiple elastic scattering (MS) using the theory of Lewis (1950), which describes the average lth-order Legendre polynomial of the scattering angle χ, is written as follows

$$\langle P_l(\cos\chi)\rangle = \mathrm{e}^{-2\pi\rho N\int_0^s\int_0^\pi \sigma_{\mathrm{el}}(T,\cos\chi)[1-P_l(\cos\theta)]\sin\theta \mathrm{d}\theta \mathrm{d}s'}, \tag{2}$$

with $\sigma_{\mathrm{el}}(T, \cos\chi)$ the elastic scattering cross section differential in solid angle, being a function of the particle energy and the cosine of the scattering angle. Note that $l = 1$ corresponds to the average cosine of the scattering angle, as $P_1(\cos\chi) = \cos\chi$. Using the continuous slowing down approximation (CSDA), as stated by equation (1), the particle energy can be entirely determined by the path in mass thickness. Therefore one can write the following

$$\langle P_l(\cos\chi)\rangle = \mathrm{e}^{-2\pi N\int_{T_i}^{T_f}\int_0^{\pi}\frac{1}{S_m(T)}\sigma_{\mathrm{el}}(T,\cos\chi)[1-P_l(\cos\theta)]\sin\theta\,\mathrm{d}\theta\,\mathrm{d}T}, \tag{3}$$

with T_i and T_f the initial and final energy defining the particle step (in mass thickness). This expression is clearly independent of the mass density. Therefore in the absence of magnetic field, one can draw the conclusion that a medium with uniform atomic properties is equivalent to particle mass-thickness trajectories to be independent of the mass density.

3.2. Violation of Fano's theorem due to external magnetic fields

Based on this representation, it is valuable to investigate how a uniform magnetic field affects the particle's mass-thickness trajectory. The change in direction from the Lorentz force can be expressed as follows (Bielajew 2001)

$$\frac{\mathrm{d}\vec{u}}{\rho\mathrm{d}s} = \frac{q}{\rho\gamma\beta mc}\vec{u}\times\vec{B}. \tag{4}$$

In this representation, the right-hand side of the equation shows a dependence on ρ. Therefore, in an arbitrary magnetic field one can conclude that the particle mass-thickness trajectory is not independent of the mass density. From the point of view of Fano's theorem, one can draw the conclusion that the presence of a uniform magnetic field is equivalent to not having uniform medium atomic properties, and therefore violating the required condition for the theorem to hold.

Figure 1 illustrates this effect in a plane perpendicular to a uniform magnetic field. The mass-thickness trajectory of a 1 MeV electron is calculated in uniform media of different densities subject to uniform transverse magnetic fields of various strengths. The transport model uses CSDA and ignores scattering effects and secondary particles, similarly to the approach of Jette (2000) without multiple scattering effects. Results show that particle trajectories significantly vary as a function of the mass density in the presence of strong magnetic fields, while this dependence diminishes as the field becomes weaker. These results are in agreement with what can be concluded from equations (1), (3) and (4).

Based on this example, one could intuitively build two special conditions where Fano's theorem is applicable in the presence of magnetic fields. One of these conditions requires a constraint on the source and is based on the rationale that the magnetic field only affects the direction of the particles. Therefore, an isotropic distribution of charged particles in equilibrium should not be perturbed by the presence of the magnetic field. It is shown in the next section that particle isotropy allows the magnetic field-dependent term of the Boltzmann transport equation to vanish, leaving the same solution as in the absence of field, independently of the field strength or direction. The second condition requires a constraint on the magnetic field. It is based on the idea of modifying the magnetic field so that mass-thickness trajectories are independent of the mass density, and therefore Fano's theorem can hold. This leaves the trivial solution where one defines a uniform magnetic field scaling proportionally to the mass density. In this case, the right-hand side of equation (4) is independent of mass density and so are the equations of motion of the mass-thickness trajectory. Figure 2 illustrates

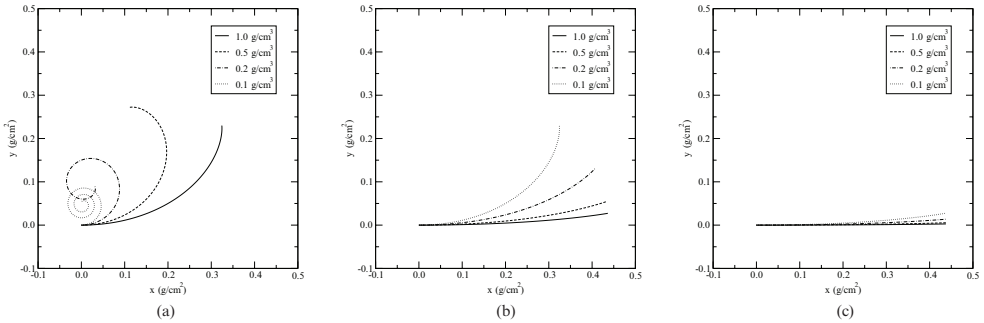

Figure 1. Mass-density dependence of the mass-thickness trajectory of a 1 MeV electron slowing down in a uniform medium subject to a transverse magnetic field: (a) $B = 1000$ mT; (b) $B = 100$ mT; (c) $B = 10$ mT.

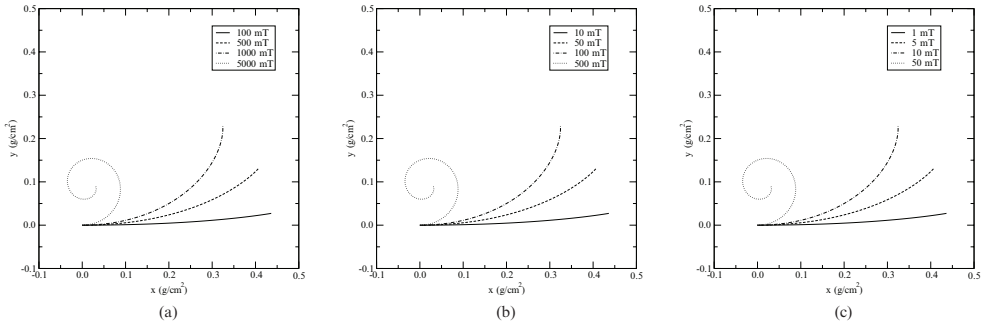

Figure 2. The impact of scaling the magnetic field with the mass density on the mass-thickness trajectory of a 1 MeV electron in different media: (a) $\rho = 1$ g cm^{-3}; (b) $\rho = 0.1$ g cm^{-3}; (c) $\rho = 0.01$ g cm^{-3}. Each of the four trajectories are identical in all three figures.

one of the two conditions, showing how scaling the field strength with the mass density yields to the same trajectory, combining several fields strengths and mass densities. A rigorous derivation of the applicability of Fano's theorem under these two special conditions is provided in the next section.

4. Special conditions for Fano's theorem to hold in external magnetic fields

To allow benchmarking Monte Carlo simulations in the presence of magnetic fields based on Fano's theorem, let us propose two conditions and demonstrate their validity in the form of theorems.

4.1. Radiation transport equations in an external magnetic field

The adapted Boltzmann transport equation for charged particle fluence in the presence of an external magnetic field $\vec{B}$ and absence of an external electric field can be written using an expression we previously derived (Bouchard and Bielajew 2015). To represent the coupled transport of photons, electrons and positrons in a medium, the following system of

equations based on coupled transport (Tervo 2007, Bouchard 2012, Bouchard *et al* 2012) is used:

$$\vec{u} \cdot \vec{\nabla}_r f_i = \rho[S_i + I_i\{f_1, f_2, f_3\}] - q_i \, \vec{u} \times \vec{B} \cdot \vec{\nabla}_p f_i \tag{5}$$

with $i = 1,2,3$, the indices representing photons, electrons and positrons, respectively, so that $q_1 = 0$ and $q_2 = -q_3$. The left-hand side of the equation equals the net amount of particles generated per unit volume at $\vec{r}$, described by the divergence of the time-integrated phase-space current density distribution $\vec{u}f_i$. On the right-hand side, the first two terms, being the source and interaction terms multiplied by the mass density, correspond to the net contribution of particles per unit volume from an external source and from interactions with the medium, respectively. The third term corresponds to the net contribution of particles per unit volume from the magnetic force and is equal to the scalar product of the magnetic force and the gradient in the momentum space of the time-integrated phase-space density distribution $\frac{1}{\beta c} f_i$.

For a fixed geometry defined by σ_{ji} and ρ, the set of particle fluences $\{f_1, f_2, f_3\}$ are uniquely determined by the set of sources $\{S_1, S_2, S_3\}$. Each interaction term I_i (in g^{-1} MeV^{-1} sr^{-1}) is an operator representing the production of particles of type i by particles of all types and is defined as follows:

$$I_i\{f_1, f_2, f_3\} = -\mu_i(p) f_i(\vec{r}, \vec{p}) + N \sum_{j=1}^{3} \int_T^{T_{\max}} \mathrm{d}T' \int_{4\pi} f_j(\vec{r}, \vec{p}\,') \sigma_{ji}(\vec{p}\,' \to \vec{p}) \mathrm{d}\vec{u}', \tag{6}$$

with $\mathrm{d}\vec{u}' = \sin\theta' \mathrm{d}\theta' \mathrm{d}\phi'$. Note here that (p, θ, ϕ) represents the vector $\vec{p}$ in spherical coordinates and $T = \sqrt{p^2c^2 - m^2c^4} - mc^2$ (with $m = 0$ for photons). On the right hand side, the first term corresponds to the loss of particles of type i with momentum $\vec{p}$, where particles of all types ($j = 1, 2, 3$) with momentum $\vec{p}\,' \neq \vec{p}$ and $p' \leqslant p$ may be produced. The second term corresponds to the gain of particles of type i with momentum $\vec{p}$, which may be produced by particles of all types ($j = 1, 2, 3$) with momentum $\vec{p}\,' \neq \vec{p}$ and $p' \geqslant p$.

4.2. Condition I: isotropic and spatially uniform sources

Theorem. *In a medium with spatially uniform atomic properties subject to a magnetic field, the particle fluences resulting from spatially uniform and isotropic primary sources are also spatially uniform and isotropic, independently of the mass density and magnetic field distributions.*

Proof. Consider a geometry with spatially uniform atomic properties such that for all interaction types, the cross sections σ_{ij} are spatially uniform and the mass density distribution is arbitrary, i.e. $\rho = \rho(\vec{r})$. Let the sources S_i be spatially uniform and isotropic but otherwise arbitrary and let $\{g_1, g_2, g_3\}$ be the fluences satisfying the following equilibrium equation system

$$S_i(p) + I_i\{g_1, g_2, g_3\} = 0 \tag{7}$$

for $i = 1, 2, 3$. Since the sources $S_i(p)$ are spatially uniform and isotropic, one would expect the solutions g_i to be also spatially uniform and isotropic, but is worth verifying this explicitly.

To show spatial uniformity, let us apply the gradient operator on equation (7), which yields

$$I_i\{\vec{\nabla}_r g_1, \vec{\nabla}_r g_2, \vec{\nabla}_r g_3\} = \vec{0}. \tag{8}$$

for $i = 1,2,3$. Note that equation (7) is scalar, while equation (8) is vectorial. But putting $S_i = 0$ in equation (7) satisfies each component of the vector equation (8), and therefore, since the solution of the equation system is unique (i.e. yielding a unique set of solutions), $\vec{\nabla}_r g_i$ are the trivial solutions for $S_i = 0$ (i.e. in the absence of sources). That is, the equilibrium solution satisfies

$$\vec{\nabla}_r g_i = \vec{0} \tag{9}$$

for $i = 1,2,3$.

To show isotropy, we make expansions in terms of orthogonal functions. This is without loss of generality because the functions being expanded are probability distributions. Let us expand g_i in spherical harmonics as follows:

$$g_i(\vec{p}) = \sum_{l=0}^{\infty} \sum_{m=-l}^{l} g_{i,l}^{m}(T) Y_l^m(\vec{u}). \tag{10}$$

Thus, one can write

$$I_i\{g_1, g_2, g_3\} = -\mu_i \sum_{l_1,m_1} g_{i,l_1}^{m_1}(T) Y_{l_1}^{m_1}(\vec{u}) + N \sum_j \sum_{l_1,m_1} \int_T^{T_{\max}} g_{j,l_1}^{m_1}(T') \mathrm{d}T' \int_{4\pi} Y_{l_1}^{m_1}(\vec{u}') \sigma_{ji}(\vec{p}' \to \vec{p}) \mathrm{d}\vec{u}'. \tag{11}$$

Using the Legendre polynomials to expand the cross sections $\sigma_{ji}(\vec{p}' \to \vec{p})$, one can write

$$\sigma_{ji}(\vec{p}' \to \vec{p}) = \sum_{l_2=0}^{\infty} a_{ji,l_2}(T' \to T) P_{l_2}(\cos\chi). \tag{12}$$

Using the addition theorem (Arfken and Weber 2011), one writes

$$P_{l_2}(\cos\chi) = \frac{4\pi}{2l_2+1} \sum_{m_2=-l_2}^{l_2} Y_{l_2}^{m_2}(\vec{u}) Y_{l_2}^{m_2 *}(\vec{u}'), \tag{13}$$

and therefore

$$\sigma_{ji}(\vec{p}' \to \vec{p}) = \sum_{l_2=0}^{\infty} \sum_{m_2=-l_2}^{l_2} \frac{4\pi}{2l_2+1} a_{ji,l_2}(T' \to T) Y_{l_2}^{m_2}(\vec{u}) Y_{l_2}^{m_2 *}(\vec{u}'). \tag{14}$$

This leads to

$$\begin{aligned} I_i\{g_1, g_2, g_3\} = &-\mu_i \sum_{l_1,m_1} g_{i,l_1}^{m_1}(T) Y_{l_1}^{m_1}(\vec{u}) \\ &+ N \sum_j \sum_{l_1,m_1} \sum_{l_2,m_2} \frac{4\pi}{2l_2+1} \int_T^{T_{\max}} a_{ji,l_2}(T' \to T) g_{j,l_1}^{m_1}(T') \mathrm{d}T' \int_{4\pi} Y_{l_1}^{m_1}(\vec{u}') Y_{l_2}^{m_2}(\vec{u}) \\ &Y_{l_2}^{m_2 *}(\vec{u}') \mathrm{d}\vec{u}'. \end{aligned} \tag{15}$$

Now let us isolate the equation for $g_{i,l}^{m}(T)$ using the orthogonality of the spherical harmonics. Let us write

$$\begin{aligned}
\int_{4\pi} I_i\{g_1,g_2,g_3\}Y_l^{m*}(\vec{u})\mathrm{d}\vec{u} &= -\mu_i \sum_{l_1,m_1} g_{i,l_1}^{m_1}(T)\int_{4\pi} Y_{l_1}^{m_1}(\vec{u})Y_l^{m*}(\vec{u})\mathrm{d}\vec{u} \\
&\quad + N\sum_j \sum_{l_1,m_1}\sum_{l_2,m_2} \frac{4\pi}{2l_2+1}\int_T^{T_{\max}} a_{ji,l_2}(T'\to T)g_{j,l_1}^{m_1}(T')\mathrm{d}T' \\
&\quad \int_{4\pi} Y_{l_2}^{m_2}(\vec{u})Y_l^{m*}(\vec{u})\mathrm{d}\vec{u}\int_{4\pi} Y_{l_1}^{m_1}(\vec{u}')Y_{l_2}^{m_2*}(\vec{u}')\mathrm{d}\vec{u}' \\
&= -\mu_i \sum_{l_1,m_1} g_{i,l_1}^{m_1}(T)\delta_{l_1 l}\delta_{m_1 m} \\
&\quad + N\sum_j \sum_{l_1,m_1}\sum_{l_2,m_2} \frac{4\pi}{2l_2+1}\int_T^{T_{\max}} a_{ji,l_2}(T'\to T)g_{j,l_1}^{m_1}(T')\mathrm{d}T' \\
&\quad \delta_{l_2 l}\delta_{m_2 m}\delta_{l_1 l_2}\delta_{m_1 m_2} \\
&= -\mu_i g_{i,l}^{m}(T) + N\sum_j \frac{4\pi}{2l+1}\int_T^{T_{\max}} a_{ji,l}(T'\to T)g_{j,l}^{m}(T')\mathrm{d}T',
\end{aligned} \tag{16}$$

for an arbitrary choice of l and m. Hence equation (7) can be transformed as follows:

$$\begin{aligned}
0 &= \int_{4\pi} S_i(p)Y_l^{m*}(\vec{u})\mathrm{d}\vec{u} + \int_{4\pi} I_i\{g_1,g_2,g_3\}Y_l^{m*}(\vec{u})\mathrm{d}\vec{u} \\
&= S_i(p)\int_{4\pi} 2\sqrt{\pi}\,Y_0^0(\vec{u})Y_l^{m*}(\vec{u})\mathrm{d}\vec{u} - \mu_i g_{i,l}^{m}(T) \\
&\quad + N\sum_j \frac{4\pi}{2l+1}\int_T^{T_{\max}} a_{ji,l}(T'\to T)g_{j,l}^{m}(T')\mathrm{d}T' \\
&= 2\sqrt{\pi}\,S_i(p)\delta_{l0}\delta_{m0} - \mu_i g_{i,l}^{m}(T) + N\sum_j \frac{4\pi}{2l+1}\int_T^{T_{\max}} a_{ji,l}(T'\to T)g_{j,l}^{m}(T')\mathrm{d}T'.
\end{aligned} \tag{17}$$

For each i, the solution $g_i(\vec{p})$ is entirely determined by $S_i(p)$. Since $g_{i,l}^{m}$ are linearly independent with l and m, the equation can be solved independently for each combination l, m. Since the source is isotropic, it is clear that $g_{i,l}^{m}=0$ satisfies the equation for all $l\neq 0$ and $m\neq 0$. Therefore, the function

$$\begin{aligned}
g_i(\vec{p}) &= \sum_{l=0}^{\infty}\sum_{m=-l}^{l} g_{i,l}^{m}(T)Y_l^m(\vec{u}) \\
&= g_{i,0}^{0}(T)Y_0^0(\vec{u}) \\
&= \frac{1}{2\sqrt{\pi}}g_{i,0}^{0}(T)
\end{aligned} \tag{18}$$

resolves equation (7) for all i and is independent of the direction $\vec{u}$. Using this result leads to

$$\vec{\nabla}_p g_i = \frac{\partial g_i}{\partial p}\vec{u} \tag{19}$$

for $i = 1, 2, 3$. Therefore, since $\vec{u} \times \vec{B}$ is perpendicular to $\vec{u}$, one can write

$$q_i \, \vec{u} \times \vec{B} \cdot \vec{\nabla}_p g_i = 0 \tag{20}$$

for all $i = 1, 2, 3$. Since the equilibrium solutions g_i satisfy the equilibrium equation system (equation (7)), they are independent of mass density, and from equations (9) and (20), they also satisfy the general transport equation system (equation (5)). □

4.3. Condition II: spatially uniform sources and density-scaled magnetic field

Theorem. *In a medium with spatially uniform atomic properties subject to an external magnetic field of fixed direction and with strength proportional to the mass density, the particle fluences resulting from spatially uniform primary sources are also spatially uniform, independently of the mass density distribution.*

Proof. Let us define the geometry with spatially uniform atomic properties such that for all interaction types, the cross sections σ_{ij} are spatially uniform and the mass density distribution is arbitrary, i.e. $\rho = \rho(\vec{r})$. Let us define the magnetic field to be given by $\vec{B} = \rho\vec{B}_m$, with $\vec{B}_m$ a constant vector, and the sources S_i to be spatially uniform with arbitrary angular distribution. Then the density ρ is a common factor to the right hand side of equation (5) and the following equilibrium equation system can be written

$$S_i(\vec{p}\,) + I_i\{g_1, g_2, g_3\} - q_i \, \vec{u} \times \vec{B}_m \cdot \vec{\nabla}_p g_i = 0 \tag{21}$$

for $i = 1, 2, 3$. Since the sources $S_i(\vec{p}\,)$ are spatially uniform, one would expect the solutions g_i to be spatially uniform. Applying the spatial gradient operator on equation (21), one obtains

$$I_i\{\vec{\nabla}_r g_1, \vec{\nabla}_r g_2, \vec{\nabla}_r g_3\} - q_i \, \vec{u} \times \vec{B}_m \cdot \vec{\nabla}_p(\vec{\nabla}_r g_i) = \vec{0} \tag{22}$$

for $i = 1, 2, 3$. Clearly this is the solution of the equation system (21) for $S_i = 0$ (i.e. the absence of sources) and therefore $\vec{\nabla}_r g_i = \vec{0}$, the solution being unique for each i. For such configuration, g_i are also solution of the equation system (5), independently of ρ. □

5. Energy deposition in special Fano cavity tests

To complete the design of the special Fano tests proposed herein, it is worth verifying that the analytic expression of energy deposition, being the typical metric used to benchmark Monte Carlo codes, is identical to Fano conditions in the absence of magnetic fields.

5.1. Condition I: spatially uniform and isotropic sources

The energy absorbed per unit mass (in Gy) is defined as the balance of interactions as follows (Bouchard 2012)

$$D = -k \sum_{i=1}^{3} \int_0^{T_{\max}} T \mathrm{d}T \int_{4\pi} I_i\{f_1, f_2, f_3\} \mathrm{d}\vec{u}, \tag{23}$$

with $k = 1.6022 \times 10^{-10}$ Gy MeV^{-1} g. Consider a geometry with uniform atomic properties subject to an arbitrary magnetic field distribution. Let us study the energy deposited locally from a set of spatially uniform and isotropic sources. We showed mathematically that this implies $\vec{\nabla}_r f_i = \vec{0}$ and $\vec{u} \times \vec{B} \cdot \vec{\nabla}_p f_i = 0$. From equation (5) one writes

$$D = k \sum_{i=1}^{3} \int_0^{T_{\max}} T \mathrm{d}T \int_{4\pi} S_i(p) \mathrm{d}\vec{u}. \tag{24}$$

For $i = 1,2,3$, let us define the source spectrum $s_i(T) = \frac{4\pi}{N_i} S_i(p)$ (in MeV^{-1}), with

$$\int_0^{T_{\max}} s_i(T) \mathrm{d}T = 1 \tag{25}$$

and N_i the number of particles emitted per unit mass in the source (in g^{-1}). The energy absorbed per unit mass (in Gy) is then given by

$$\begin{aligned} D &= k \sum_{i=1}^{3} N_i \int_0^{T_{\max}} s_i(T) T \mathrm{d}T \\ &= k \sum_{i=1}^{3} N_i \langle T \rangle_i. \end{aligned} \tag{26}$$

with $\langle T \rangle_i$ the average kinetic energy (in MeV) over the source of particles of type i. Note that this result is independent of the magnetic field distribution and therefore is the same in the absence of magnetic fields, i.e. such as in a standard Fano test. It is also worth noting that in the case of photons being used to generate electrons through their interactions, this relation equals collision kerma. If electrons are generated randomly by a spontaneous source, N_i and $\langle T \rangle_i$ must be defined as a simulation input.

5.2. Condition II: spatially uniform sources and density-scaled magnetic fields

Allow a geometry with uniform atomic properties subject to a magnetic field of constant direction and strength proportional to the mass density, i.e. $\vec{B} = \rho \vec{B}_m$, with $\vec{B}_m$ a constant vector. Let us study the case where the sources are spatially uniform with arbitrary angular distribution. Since $\vec{\nabla}_r f_i = \vec{0}$, from equation (5) and (23) one finds

$$D = k \sum_{i=1}^{3} \int_0^{T_{\max}} T \mathrm{d}T \int_{4\pi} S_i(\vec{p}) \mathrm{d}\vec{u} - k \sum_{i=1}^{3} q_i \int_0^{T_{\max}} T \mathrm{d}T \int_{4\pi} \vec{u} \times \vec{B}_m \cdot \vec{\nabla}_p f_i \, \mathrm{d}\vec{u}. \tag{27}$$

On the right hand side of the equation, the first term results in equation (26) by defining the source spectra for $i = 1,2,3$ as

$$s_i(T) = \frac{1}{N_i} \int_{4\pi} S_i(\vec{p}) \mathrm{d}\vec{u}. \tag{28}$$

Note that this general definition can also be applied for an isotropic source, yielding $s_i(T) = \frac{4\pi}{N_i} S_i(p)$ as in condition I. The second term of equation (27) can be shown to vanish using spherical coordinates of $\vec{p}$ and the following integrals for $i = 1,2,3$. First, expressing the gradient in the momentum space yields

$$\int_{4\pi} \vec{u} \times \vec{B}_m \cdot \vec{\nabla}_p f_i \, \mathrm{d}\vec{u} = \int_{4\pi} \vec{u} \times \vec{B}_m \cdot \vec{u} \, \frac{\partial f_i}{\partial p} \mathrm{d}\vec{u} + \int_{4\pi} \vec{u} \times \vec{B}_m \cdot \hat{\theta} \, \frac{1}{p} \frac{\partial f_i}{\partial \theta} \, \mathrm{d}\vec{u} + \int_{4\pi} \vec{u} \times \vec{B}_m \cdot \hat{\phi} \, \frac{1}{p \sin\theta} \frac{\partial f_i}{\partial \phi} \, \mathrm{d}\vec{u}. \tag{29}$$

Clearly, the first term on the right-hand side of the equation vanishes. Using the properties of the scalar triple product, one obtains

$$\int_{4\pi} \vec{u} \times \vec{B}_m \cdot \vec{\nabla}_p f_i \, \mathrm{d}\vec{u} = \int_{4\pi} \hat{\theta} \times \vec{u} \cdot \vec{B}_m \, \frac{1}{p} \frac{\partial f_i}{\partial \theta} \, \mathrm{d}\vec{u} + \int_{4\pi} \hat{\phi} \times \vec{u} \cdot \vec{B}_m \, \frac{1}{p \sin\theta} \frac{\partial f_i}{\partial \phi} \, \mathrm{d}\vec{u}, \tag{30}$$

which yields to

$$\int_{4\pi} \vec{u} \times \vec{B}_m \cdot \vec{\nabla}_p f_i \, \mathrm{d}\vec{u} = -\frac{1}{p} \vec{B}_m \cdot \int_{4\pi} \hat{\phi} \, \frac{\partial f_i}{\partial \theta} \, \mathrm{d}\vec{u} + \frac{1}{p} \vec{B}_m \cdot \int_{4\pi} \hat{\theta} \, \frac{1}{\sin\theta} \frac{\partial f_i}{\partial \phi} \, \mathrm{d}\vec{u}. \tag{31}$$

Expressing the resulting vectors in the spatial coordinates as follows

$$\int_{4\pi} \vec{u} \times \vec{B}_m \cdot \vec{\nabla}_p f_i \, \mathrm{d}\vec{u} = \frac{1}{p} \vec{B}_m \cdot \int_0^{2\pi} \mathrm{d}\phi \int_0^{\pi} (\sin\theta \sin\phi \hat{x} - \sin\theta \cos\phi \hat{y}) \, \frac{\partial f_i}{\partial \theta} \, \mathrm{d}\theta + \frac{1}{p} \vec{B}_m \cdot \int_0^{\pi} \mathrm{d}\theta \int_0^{2\pi} (\cos\theta \cos\phi \hat{x} + \cos\theta \sin\phi \hat{y} - \sin\theta \hat{z}) \, \frac{\partial f_i}{\partial \phi} \, \mathrm{d}\phi. \tag{32}$$

Finally, integrating the right-hand side of the equation by part yields

$$\begin{aligned} \int_{4\pi} \vec{u} \times \vec{B}_m \cdot \vec{\nabla}_p f_i \, \mathrm{d}\vec{u} &= -\frac{1}{p} \vec{B}_m \cdot \int_0^{2\pi} \mathrm{d}\phi \int_0^{\pi} (\cos\theta \sin\phi \hat{x} - \cos\theta \cos\phi \hat{y}) f_i \, \mathrm{d}\theta \\ &\quad -\frac{1}{p} \vec{B}_m \cdot \int_0^{\pi} \mathrm{d}\theta \int_0^{2\pi} (-\cos\theta \sin\phi \hat{x} + \cos\theta \cos\phi \hat{y}) f_i \, \mathrm{d}\phi \\ &= 0. \end{aligned} \tag{33}$$

Therefore, equation (26) also applies in this case as the magnetic field does not affect the energy deposition.

6. Conclusion

The present study proposes special conditions under which the Fano theorem remains valid in the presence of an external magnetic field. The first condition requires a spatially uniform and isotropic source and is valid for any magnetic field distribution. The second condition requires a spatially uniform source and a magnetic field distribution with constant direction and strength proportional to the mass density of the media. In both cases, the expression for absorbed dose takes the same form as it does in the standard conditions under which Fano's theorem applies, i.e. in the absence of a magnetic field. An important application of these special conditions is

the implementation of novel benchmark tests (i.e. special Fano cavity tests) for the Monte Carlo simulation of radiation transport with magnetic fields. We expect that this work is a crucial step towards accurate detector dose response simulation in the context of MRI-guided radiotherapy, and therefore will impact the clinical calibration of such new beams in the future.

Acknowledgments

We are grateful to Professor P Andreo for sharing an early version of an upcoming book entitled Fundamentals of Ionizing Radiation Dosimetry (FIORD), which provided helpful definitions used in this work.

References

Alfonso R *et al* 2008 A new formalism for reference dosimetry of small and nonstandard fields *Med. Phys.* **35** 5179–86

Almond P R, Biggs P J, Coursey B M, Hanson W F, Huq M S, Nath R and Rogers D W O 1999 AAPM's TG-51 protocol for clinical reference dosimetry of high-energy photon and electron beams *Med. Phys.* **26** 1847–69

Andreo P and Brahme A 1986 Stopping power data for high-energy photon beam *Phys. Med. Biol.* **31** 839–58

Andreo P, Burns D T, Hohfield K, Huq M S, Kanai T, Laitano F, Smyth V and Vynckier S 2001 Absorbed dose determination in external beam radiotherapy: an international code of practice for dosimetry based on standards of absorbed dose to water *Technical Report* TRS-398 (Austria: International Atomic Energy Agency Vienna)

Andreo P 1994 Improved calculations of stopping-power ratios and their correlation with the quality of therapeutic photon beams *Measurement Assurance in Dosimetry (Proc. Symp. Vienna)* (Vienna: IAEA) pp 335–59

Arfken G B and Weber H J 2011 *Mathematical Methods for Physicists: A Comprehensive Guide* (New York: Academic)

Benmakhlouf H, Sempau J and Andreo P 2014 Output correction factors for nine small field detectors in 6 MV radiation therapy photon beams: a PENELOPE Monte Carlo study *Med. Phys.* **41** 041711

Bielajew A F 1990a An analytic theory of the point-source nonuniformity correction factor for thick-walled ionisation chambers in photon beams *Phys. Med. Biol.* **35** 517

Bielajew A F 1990b Correction factors for thick-walled ionisation chambers in point-source photon beams *Phys. Med. Biol.* **35** 501

Bielajew A F 2001 Fundamentals of the monte carlo method for neutral and charged particle transport *The University of Michigan*

Bouchard H 2012 A theoretical re-examination of Spencer–Attix cavity theory *Phys. Med. Biol.* **57** 3333

Bouchard H and Bielajew A 2014 A theoretical framework to improve Monte Carlo algorithms coupled to magnetic fields *International Workshop on Monte Carlo Techniques in Medical Physics* (*Program and Abstracts*) vol 1 (Québec: Université Laval) p 17

Bouchard H and Bielajew A 2015 Lorentz force correction to the Boltzmann radiation transport equation and its implications for Monte Carlo algorithms *Phys. Med. Biol.* **60** 4963–72

Bouchard H, Seuntjens J and Palmans H 2012 On charged particle equilibrium violation in external photon fields *Med. Phys.* **39** 1473–80

Cranmer-Sargison G, Weston S, Evans J, Sidhu N and Thwaites D 2012 Monte Carlo modelling of diode detectors for small field MV photon dosimetry: detector model simplification and the sensitivity of correction factors to source parameterization *Phys. Med. Biol.* **57** 5141

Czarnecki D and Zink K 2013 Monte Carlo calculated correction factors for diodes and ion chambers in small photon fields *Phys. Med. Biol.* **58** 2431

Elles S, Ivanchenko V, Maire M and Urban L 2008 Geant4 and Fano cavity test: where are we? *J. Phys.: Conf. Ser.* **102** 012009

Fano U 1954 Note on the Bragg–Gray cavity principle for measuring energy dissipation *Radiation Res.* **1** 237–40

Foote B and Smyth V 1995 The modelling of electron multiple scattering in EGS4/PRESTA and its effect on ionisation chamber response *Nucl. Instrum. Methods Phys. Res.* **100** 22–30

Francescon P, Beddar S, Satariano N and Das I J 2014a Variation of $k_{Q_{\text{clin}},Q_{\text{msr}}}^{f_{\text{clin}},f_{\text{msr}}}$ for the small-field dosimetric parameters percentage depth dose, tissue-maximum ratio, and off-axis ratio *Med. Phys.* **41** 101708

Francescon P, Cora S and Cavedon C 2008 Total scatter factors of small beams: a multidetector and Monte Carlo study *Med.Phys.* **35** 504–13

Francescon P, Cora S and Satariano N 2011 Calculation of $k_{Q_{\text{clin}},Q_{\text{msr}}}^{f_{\text{clin}},f_{\text{msr}}}$ for several small detectors and for two linear accelerators using Monte Carlo simulations *Med. Phys.* **38** 6513–27

Francescon P, Kilby W, Satariano N and Cora S 2012 Monte Carlo simulated correction factors for machine specific reference field dose calibration and output factor measurement using fixed and iris collimators on the cyberknife system *Phys. Med. Biol.* **57** 3741

Francescon P, Kilby W and Satariano N 2014b Monte Carlo simulated correction factors for output factor measurement with the CyberKnife system-results for new detectors and correction factor dependence on measurement distance and detector orientation *Phys. Med. Biol.* **59** N11

Gago-Arias A, Rodriguez-Romero R, Sánchez-Rubio P, González-Casta D M, Gómez F, Núñez L, Palmans H, Sharpe P and Pardo-Montero J 2012 Correction factors for A1Sl ionization chamber dosimetry in tomotherapy: machine-specific, plan-class, and clinical fields *Med. Phys.* **39** 1964–70

Jette D 2000 Magnetic fields with photon beams: Monte Carlo calculations for a model magnetic field *Med. Phys.* **27** 2726–38

Kamio Y and Bouchard H 2014 Correction-less dosimetry of nonstandard photon fields: a new criterion to determine the usability of radiation detectors *Phys. Med. Biol.* **59** 4973

Kawrakow I 2000a Accurate condensed history Monte Carlo simulation of electron transport. I. EGSnrc, the new EGS4 version *Med. Phys.* **27** 485–98

Kawrakow I 2000b Accurate condensed history Monte Carlo simulation of electron transport. II. Application to ion chamber response simulations *Med. Phys.* **27** 499–513

Kosunen A and Rogers D 1993 Beam quality specification for photon beam dosimetry *Med. Phys.* **20** 1181–8

Lewis H 1950 Multiple scattering in an infinite medium *Phys. Rev.* **78** 526

McEwen M, DeWerd L, Ibbott G, Followill D, Rogers D W, Seltzer S and Seuntjens J 2014 Addendum to the AAPM's TG-51 protocol for clinical reference dosimetry of high-energy photon beams *Med. Phys.* **41** 041501

Meijsing I, Raaymakers B, Raaijmakers A, Kok J, Hogeweg L, Liu B and Lagendijk J 2009 Dosimetry for the MRI accelerator: the impact of a magnetic field on the response of a Farmer NE2571 ionization chamber *Phys. Med. Biol.* **54** 2993

Muir B, McEwen M and Rogers D 2011 Measured and Monte Carlo calculated kq factors: accuracy and comparison *Med. Phys.* **38** 4600–9

Muir B and Rogers D 2010 Monte Carlo calculations of kq, the beam quality conversion factor *Med. Phys.* **37** 5939–50

Papaconstadopoulos P, Tessier F and Seuntjens J 2014 On the correction, perturbation and modification of small field detectors in relative dosimetry *Phys. Med. Biol.* **59** 5937

Poon E and Verhaegen F 2005 Accuracy of the photon and electron physics in geant4 for radiotherapy applications *Med. Phys.* **32** 1696–711

Reynolds M, Fallone B and Rathee S 2013 Dose response of selected ion chambers in applied homogeneous transverse and longitudinal magnetic fields *Med. Phys.* **40** 042102

Rogers D and Yang C 1999 Corrected relationship between $\%dd(10)_x$ and stopping-power ratios *Med. Phys.* **26** 538–40

Scott A J, Kumar S, Nahum A E and Fenwick J D 2012 Characterizing the influence of detector density on dosimeter response in non-equilibrium small photon fields *Phys. Med. Biol.* **57** 4461

Scott A J, Nahum A E and Fenwick J D 2008 Using a Monte Carlo model to predict dosimetric properties of small radiotherapy photon fields *Med. Phys.* **35** 4671–84

Sempau J and Andreo P 2006 Configuration of the electron transport algorithm of PENELOPE to simulate ion chambers *Phys. Med. Biol.* **51** 3533

Seuntjens J, Kawrakow I, Borg J, Hobeila F and Rogers D 2002 Calculated and measured air-kerma response of ionization chambers in low and medium energy photon beams *Proc. of an Int. Monte Carlo Workshop* pp 69–84

Smit K, Van Asselen B, Kok J, Aalbers A, Lagendijk J and Raaymakers B 2013 Towards reference dosimetry for the mr-linac: magnetic field correction of the ionization chamber reading *Phys. Med. Biol.* **58** 5945

Smyth V G 1986 Interface effects in the Monte Carlo simulation of electron tracks *Med. Phys.* **13** 196–200

Sterpin E, Mackie T R and Vynckier S 2012 Monte Carlo computed machine-specific correction factors for reference dosimetry of tomotherapy static beam for several ion chambers *Med. Phys.* **39** 4066–72

Sterpin E, Sorriaux J, Souris K, Vynckier S and Bouchard H 2014 A Fano cavity test for Monte Carlo proton transport algorithms *Med. Phys.* **41** 011706

Tervo J 2007 On coupled boltzmann transport equation related to radiation therapy *J. Math. Anal. Appl.* **335** 819–40

Underwood T, Winter H, Hill M and Fenwick J 2013 Detector density and small field dosimetry: integral versus point dose measurement schemes *Med. Phys.* **40** 082102

Yi C Y, Hah S H and Yeom M S 2006 Monte Carlo calculation of the ionization chamber response to Co-60 beam using PENELOPE *Med. Phys.* **33** 1213–21